Epidemiol. Infect. (2007), **135**, 281–292. © 2006 Cambridge University Press
doi:10.1017/S0950268806006698 Printed in the United Kingdom

Seasonality in six enterically transmitted diseases and ambient temperature

E. N. NAUMOVA[1]*, J. S. JAGAI[1], B. MATYAS[2], A. DEMARIA JR.[2], I. B. MACNEILL[3] AND J. K. GRIFFITHS[1]

[1] *Tufts University School of Medicine, Boston, MA, USA*
[2] *Massachusetts Department of Public Health, Boston, MA, USA*
[3] *University of Western Ontario, London, Canada*

(*Accepted 3 April 2006; first published online 19 June 2006*)

SUMMARY

We propose an analytical and conceptual framework for a systematic and comprehensive assessment of disease seasonality to detect changes and to quantify and compare temporal patterns. To demonstrate the proposed technique, we examined seasonal patterns of six enterically transmitted reportable diseases (EDs) in Massachusetts collected over a 10-year period (1992–2001). We quantified the timing and intensity of seasonal peaks of ED incidence and examined the synchronization in timing of these peaks with respect to ambient temperature. All EDs, except hepatitis A, exhibited well-defined seasonal patterns which clustered into two groups. The peak in daily incidence of *Campylobacter* and *Salmonella* closely followed the peak in ambient temperature with the lag of 2–14 days. *Cryptosporidium*, *Shigella*, and *Giardia* exhibited significant delays relative to the peak in temperature ($\sim$40 days, $P<0{\cdot}02$). The proposed approach provides a detailed quantification of seasonality that enabled us to detect significant differences in the seasonal peaks of enteric infections which would have been lost in an analysis using monthly or weekly cumulative information. This highly relevant to disease surveillance approach can be used to generate and test hypotheses related to disease seasonality and potential routes of transmission with respect to environmental factors.

INTRODUCTION

In temperate climates, waterborne or foodborne enteric infections typically alternate periods of low endemic levels with periods with outbreaks, forming a typical seasonal pattern. For example, illness caused by *Salmonella* spp. or *Campylobacter jejuni* rises in the summer and declines in the winter [1–7]. Enteric infections caused by the protozoans *Giardia* and *Cryptosporidium* also exhibit seasonal variation, although shifted towards autumn [8–14]. In contrast, hepatitis A and shigellosis seasonality is not marked [4].

Consistent temporal fluctuations for diseases with similar sources for exposure or similar routes of transmission, suggest the presence of environmental factors that synchronize seasonal variation [15]. Deviations from an established seasonal pattern may provide important clues to the factors that influence disease occurrence. These factors may include changes in the sources of exposure and spread, changes in the affected population, or differences in the pathogen itself. Ecological disturbances, perhaps from climate

* Author for correspondence: E. N. Naumova, Ph.D., Associate Professor, Department of Public Health and Family Medicine, Tufts University School of Medicine, 136 Harrison Ave, Boston, MA 02111, USA.
(Email: elena.naumova@tufts.edu)

Table 1. *Proposed characteristics to describe seasonality for exposure and outcome variables*

Proposed characteristics describing seasonality	For exposure (e.g. average ambient temperature)	For outcome (e.g. reported enteric disease incidence)
Average maximum value – seasonal peak	$\max\{Y(t)\}=\beta_0+\gamma$	$\max\{Y(t)\}=\exp\{\beta_0+\gamma\}$
Average minimum value – seasonal nadir	$\min\{Y(t)\}=\beta_0-\gamma$	$\min\{Y(t)\}=\exp\{\beta_0-\gamma\}$
Average intensity – the difference between maximum and minimum values	$I=2\gamma$	$I=\exp\{\beta_0+\gamma\}-\exp\{\beta_0-\gamma\}$
Average relative intensity – the ratio of the maximum and minimum values on the seasonal curve	$I_R=(\beta_0^2-\gamma^2)/(\beta_0-\gamma)^2$	$I_R=\exp\{2\gamma\}$
Average peak timing – the temporal position of the maximum point on the seasonal curve (expressed in days)	$P_E=365(1-\psi/\pi)/2$	$P_D=365(1-\psi/\pi)/2$
Average lag – the difference between the peak time of exposure and the peak timing of disease incidence	P_E-P_D	

change, may influence the emergence and proliferation of parasitic diseases, including cryptosporidiosis and giardiasis [16]. Ambient temperature has been associated with short-term temporal variations (week-to-week and month-to-month) in reported cases of food poisoning in the United Kingdom, often caused by *Salmonella* [17–20]. Increased temperatures and extreme precipitation events have also been shown to have a short-term effect on health outcomes [21–23]. To quote Epstein [24], 'climate constrains the range of infectious diseases, while weather affects the timing and intensity of outbreaks'. It is plausible that the temporal pattern in ambient temperature may determine, in part, the timing and magnitude of the peak of a disease incidence curve for specific enteric diseases.

An understanding of how specific environmental factors influence human disease may improve disease forecasting, enhance the design of integrated warning systems, and advance the development of efficient outbreak detection algorithms. Although seasonality is a well-known characteristic of enteric infections, simple analytical tools for the examination, evaluation, and comparison of seasonal patterns are limited. Herein, we offer a framework for seasonality assessment, and a parametric approach for seasonality evaluation. We contrast our approach with non-parametric modelling. To demonstrate the proposed method, while providing step-by-step instructions for implementation, we examine the variability in seasonality of six enteric diseases with respect to ambient temperature in the temperate climate of Massachusetts (MA) over the last decade. We consider two parasite infections (*Giardia* and *Cryptosporidium*), three bacterial infections (*Salmonella*, *Campylobacter* and *Shigella*), and one viral disease, hepatitis A. All of these enteric infections can be waterborne and/or foodborne, have low endemic winter incidence rates and localized outbreaks, typically exhibit a yearly summer or autumn peak, and are diseases reportable to the Massachusetts Department of Public Health (MDPH).

METHODS

Data abstraction

We abstracted all reported laboratory-confirmed cases (45 816 records, without personal identifiers) for six diseases: giardiasis, cryptosporidiosis, salmonellosis, campylobacteriosis, shigellosis, and hepatitis A. The number of cases by disease is shown in Table 1. The abstraction covers all of MA over a 10-year period (3653 days) from 1 January 1992 to 31 December 2001. Criteria for reportable cases to MDPH include: for cryptosporidiosis and giardiasis – demonstration of *Cryptosporidium* oocysts or *Giardia lamblia* cysts in stool; demonstration of *Cryptosporidium* or *G. lamblia* cysts in intestinal fluid or small-bowel biopsy specimens; or demonstration of *Cryptosporidium* or *G. lamblia* antigen in stool by a specific immunodiagnostic test [e.g. enzyme-linked immunosorbent assay (ELISA)]; for salmonellosis (non-typhoid) and shigellosis – isolation of *Salmonella* or *Shigella* species from any clinical specimen; for hepatitis A – serological evidence of recent hepatitis A virus infection (anti-hepatitis A IgM antibody) associated with a consistent clinical syndrome, or known exposure to an infectious case with or without symptoms in the contact. For each reported case, variables necessary for spatial and temporal analysis were

obtained: sex, age, zip code of residence, and dates of disease onset and reporting. Using the date of disease onset, the time series of daily counts of reported laboratory-confirmed cases of the six enteric diseases (EDs) were created.

Daily ambient temperature records from 38 MA monitoring stations were abstracted from the National Climatic Data Center (NCDC) Summary of the Day database (EarthInfo Inc., Boulder, CO, USA). A daily average of recorded maximum temperature was calculated from all active stations. On any given day, data were available from at least 94% of stations. Of the 14 MA counties, 12 counties had from 1 to 6 active stations. The counties with the most stations [Worcester (6), Essex (5), Middlesex (5), and Plymouth (5)] include half of MA's population. The two counties without stations, Franklin and Nantucket, are among the least densely populated in the state. A time series of the daily averaged maximum ambient temperature was created.

Conceptual framework for seasonality assessment

We define 'seasonality' as systematic, or repetitive, periodic fluctuations in a variable of interest (i.e. disease incidence or environmental exposure, e.g. temperature) that occur within the course of a year. It can be characterized by the magnitude, timing, and duration of a seasonal increase. We define the *time of the seasonal peak*, a parameter of interest, as the position of the maximum point on the seasonal curve. The maximum and minimum values on the seasonal curve, the difference between, and the ratio of these values are the *magnitude*-related measures. The conceptual framework for measuring the temporal relation between seasonal patterns in environmental temperatures and disease incidence is shown on Figure 1. The *synchronization* in disease incidence and environmental factors can be viewed as a special case when multiple time series exhibit common periodicities [25] and can be characterized, in part, by a lag, a difference between peak timing in disease incidence and exposure.

This conceptual framework is expressed via model (1) as follows:

$$Y(t)=\gamma\ \cos(2\pi\omega t+\psi)+e(t), \tag{1}$$

where $Y(t)$ is a time series; the periodic component has a frequency of ω, an amplitude of γ, and a phase angle of ψ; and $\{e(t),\ t=1, 2, \ldots, n\}$ is an i.i.d. sequence of random variables with $E[e(t)]=0$ and $\mathrm{Var}[e(t)]=\sigma^2$. This easy-to-interpret model describes a seasonal curve by a cosine function with symmetric rise and fall over a period of a full year. The locations of two points, the seasonal curve peak and nadir, can be determined using a shift, or phase angle parameter, ψ, which reflects the timing of the peak relative to the origin. If $\psi=1$, there is no shift of the peak relative to the origin, and the curve peaks in the summer on the 182nd day; if $1<\psi<2$ then there is a shift towards autumn; and if $0<\psi<1$ then the shift is towards spring. For convenience, an origin can be set at the calendar year beginning 1 January, but it can be also reset at any other day. The shift parameter can be expressed in days and used for seasonality comparison. The amplitude of fluctuations between two extreme points is controlled via parameter γ. If $\gamma=0$, there is no seasonal increase. Estimates of model (1) are difficult to obtain because both ψ and γ are unknown, but its equivalent model (2):

$$Y(t)=\beta_1 \sin(2\pi\omega t)+\beta_2 \cos(2\pi\omega t)+e(t), \tag{2}$$

is easy to fit by the least squares procedure available in commercial statistical software programs. Elsewhere, we have proposed an approach, which allows us to combine the ease of fitting model (2) and the simplicity and elegance of interpretation of model (1), by using the δ-method [26]. We demonstrated that estimates of the amplitude and shift parameters of model (1) can be obtained from the estimates of model (2): for the amplitude, the estimates of the mean and variance are

$$\hat{\gamma}=f(\hat{\beta}_1, \hat{\beta}_2)=\delta(\hat{\beta}_1^2+\hat{\beta}_2^2)^{\frac{1}{2}},$$

where $\delta=1$, if $\beta_2>0$, and $\delta=-1$, if $\beta_2<0$ and

$$\mathrm{Var}(\hat{\gamma})=(\hat{\sigma}^2_{\beta_1}\hat{\beta}_1^2+\hat{\sigma}^2_{\beta_2}\hat{\beta}_2^2+2\hat{\sigma}_{\beta_1\beta_2}\hat{\beta}_1\hat{\beta}_2)/(\hat{\beta}_1^2+\hat{\beta}_2^2),$$

and the phase angle estimates are

$$\hat{\psi}=-\arctan(\hat{\beta}_1/\hat{\beta}_2) \text{ and}$$

$$\mathrm{Var}(\hat{\psi})=(\hat{\sigma}^2_{\beta_1}\hat{\beta}_2^2+\hat{\sigma}^2_{\beta_2}\hat{\beta}_1^2-2\hat{\sigma}_{\beta_1\beta_2}\hat{\beta}_1\hat{\beta}_2)/(\hat{\beta}_1^2+\hat{\beta}_2^2)^2.$$

Parametric modelling procedures

To describe the seasonal pattern in the daily time series of temperature and infections and estimate its parameters, we used generalized linear models (GLM) with a Gaussian distribution for ambient temperature as the outcome variable of interest using model A:

$$Y(t)=\beta_0+\beta_1 \sin(2\pi\omega t)+\beta_2 \cos(2\pi\omega t)+e(t), \tag{3}$$

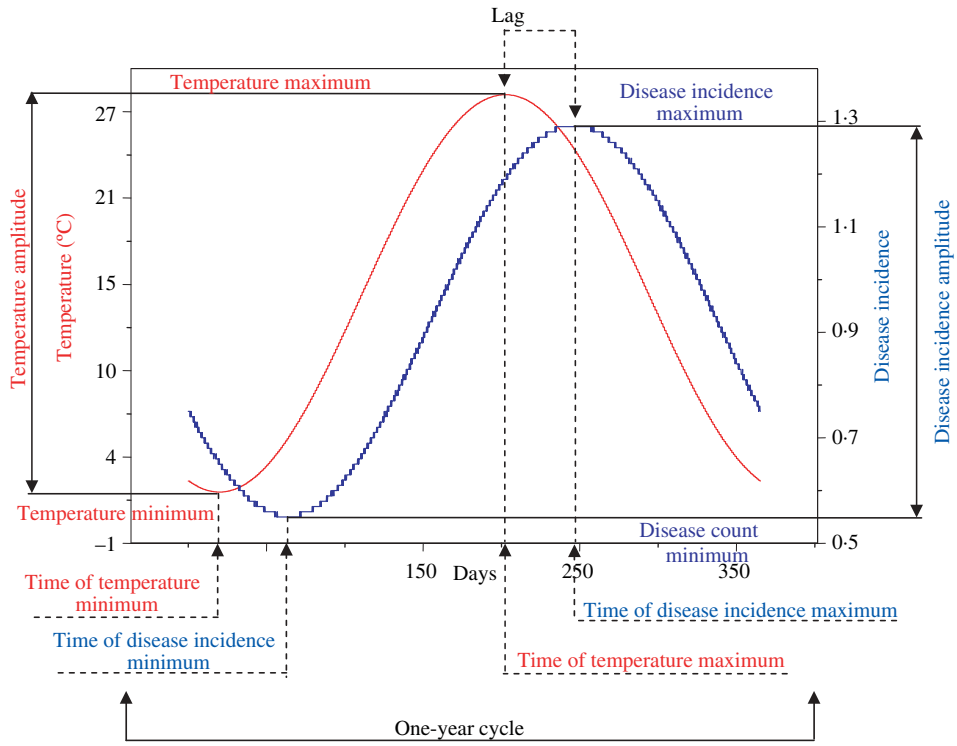

Characteristics		Definition	Units
Timing	Maximum	Position of maximum point on the seasonal curve of temperature or disease incidence	Days
	Minimum	Position of minimum point on the seasonal curve of temperature or disease incidence	Days
	Lag	Difference between time of temperature maximum and time of disease incidence maximum	Days
Intensity	Maximum	Maximum value on seasonal curve of temperature or disease incidence	Degrees/Cases
	Minimum	Minimum value on seasonal curve of temperature or disease incidence	Degrees/Cases
	Amplitude	Difference between maximum and minimum of seasonal curve for temperature or disease incidence	Degrees/Cases
	Magnitude	Ratio of maximum value divided by minimum value of the seasonal curve	Unit-less

Fig. 1. Characteristics of seasonality: Graphical depiction and definition for daily time series of exposure (ambient temperature) and outcome (disease incidence) variables. The red labels are related to exposure measures and the blue labels are related to disease incidence measures.

and a Poisson distribution if the studied outcome is daily disease counts, model B:

$$\log[Y(t)] = \beta_0 + \beta_1 \sin(2\pi\omega t) + \beta_2 \cos(2\pi\omega t) + e(t). \tag{4}$$

In both models, β_0 is an intercept, a baseline of a seasonal pattern, and t is time in days ($t = 1, 2, \ldots, N$, where N is the number of days in a time series). To properly express the frequency, we set $\omega = 1/N$. The $\exp\{\beta_0\}$ for the Poisson regression reflects mean daily disease counts over a study period. Using the estimates of the amplitude and the phase angle, we may now propose seasonality characteristics to help us in assessing seasonality. They are listed in Table 1, and include: the average maximum value (of either exposure or disease incidence), the average minimum value, their absolute and relative intensities, the average peak timing in days, and the average lag period in days between peak exposure and peak disease incidence. Importantly, by using estimates of the variance for the amplitude and the phase angle parameters, the upper and lower confidence intervals can be also estimated for all proposed characteristics.

Table 2. *Reported laboratory-confirmed infections and their seasonal characteristics*

	Temperature (°C/day)	Campylo-bacteriosis	Salmonellosis	Shigellosis	Crypto-sporidiosis	Giardiasis	Hepatitis A
Total cases		14 992	15 518	3202	528	9504	2072
Mean ± S.D.	14·97 ± 9·92	4·10 ± 3·02	4·25 ± 3·33	0·88 ± 1·31	0·14 ± 0·48	2·60 ± 2·57	0·57 ± 0·86
1st, 3rd quartile	(6·6, 23·8)	(2, 5)	(2, 6)	(0, 1)	(0, 0)	(1, 4)	(0, 1)
Maximum	34·56	26	32	13	9	22	7
	Model A	Model B					
Predicted							
Min, max value	(2·2, 27·8)	(2·55, 6·03)	(2·32, 6·75)	(0·46, 1·42)	(0·06, 0·28)	(1·74, 3·64)	(0·46, 0·69)
Average intensity	7·78	3·47	4·43	0·96	0·22	1·91	0·23
Relative intensity	2·28	2·36	2·91	3·07	5·00	2·10	1·49
Peak (days)	206 ± 0·22	208 ± 0·79	219 ± 0·30	247 ± 1·26	242 ± 1·73	249 ± 1·18	269 ± 9·81
LCI, UCI (days)	(206–207)	(206–209)	(218–219)	(245–250)	(239–246)	(247–251)	(249–288)
Variation explained by seasonality	83 %	17 %	23 %	8 %	6 %	8 %	1 %

LCI, lower confidence interval; UCI, upper confidence interval.

Non-parametric modelling procedures

As the basis for comparisons of models A and B to a commonly used in epidemiology approach, we applied a model that includes a set of indicator variables to reflect a week of the year and adapts the Gaussian or Poisson distributions as an outcome's distributional assumption [27]:

$$Y(t) = \beta_0 + \beta_i X_i + e(t), \qquad \text{(Model C)}$$

or

$$\log[Y(t)] = \beta_0 + \beta_i X_i + e(t), \qquad \text{(Model D)}$$

where $Y = \{y_1, y_2, \ldots, y_N\}$, is a time series of daily counts or daily temperature, X is a matrix of indicator variables for a week of observation, β_i are slopes for a corresponding indicator of a week (for $i = 2, \ldots, 53$), β_0 is an mean value for the reference week (in our case, the first week of the year), and ε is an error term. Based on regression parameters of model D, we estimated a predicted number of cases for a given week, e.g. $Y_0^* = \exp\{\beta_0\}$ is an estimate at week 1; $Y_i^* = \exp\{\beta_0 + \beta_i\}$ is an estimate at week i. For each estimate, we calculated a corresponding 95% confidence interval, 95% CI $= \exp\{\beta_0 + \beta_i \pm 1{\cdot}96(S_{\beta_0} + S_{\beta_i})/2\}$, where S_{β_i} is a standard error of a regression parameter β_i. To describe a period of seasonal increase we determined weeks with high rates: if the predicted number of cases for i week, R_i, had a value less than a pre-specified cut point, R_c, then we assigned this week to a period of seasonal increase. We selected three cut points as the 75th, 85th, and 95th percentiles of a distribution of predicted weekly incidence. Similar estimations, except for exponentiation, were performed for the temperature (model C).

For each model and each ED the percent of variance explained was calculated. All analysis was performed using S-plus 4.5 (Insightful Corp., Seattle, WA, USA) statistical software.

RESULTS

Three-dimensional scatter plots with superimposed linear regression surfaces were created to illustrate temperature–ED incidence relations over time (Fig. 2). These show 10-year trends in disease incidence, with respect to daily ambient temperature. The annual summer disease increase is far more pronounced than any of the annual trends for the six EDs. The time series of daily values of ambient temperature is shown in Figure 3*a*.

Descriptive statistics of laboratory-confirmed reported cases for all six EDs are shown in Table 2: total number of cases, daily mean with standard deviation, the range (expressed as 25th and 75th percentiles), and the maximum observable number of cases per day. *Salmonella*, *Campylobacter*, and *Giardia* are the most commonly reported EDs in MA. Due to outbreaks, the range of daily fluctuation is poorly captured by the 25th and 75th percentiles, and the difference between the daily maximum and the daily mean typically exceeds seven standard deviations. Reporting of *Cryptosporidium* was low until 1995, when an unusual number of cryptosporidiosis cases were diagnosed in Worcester, MA.

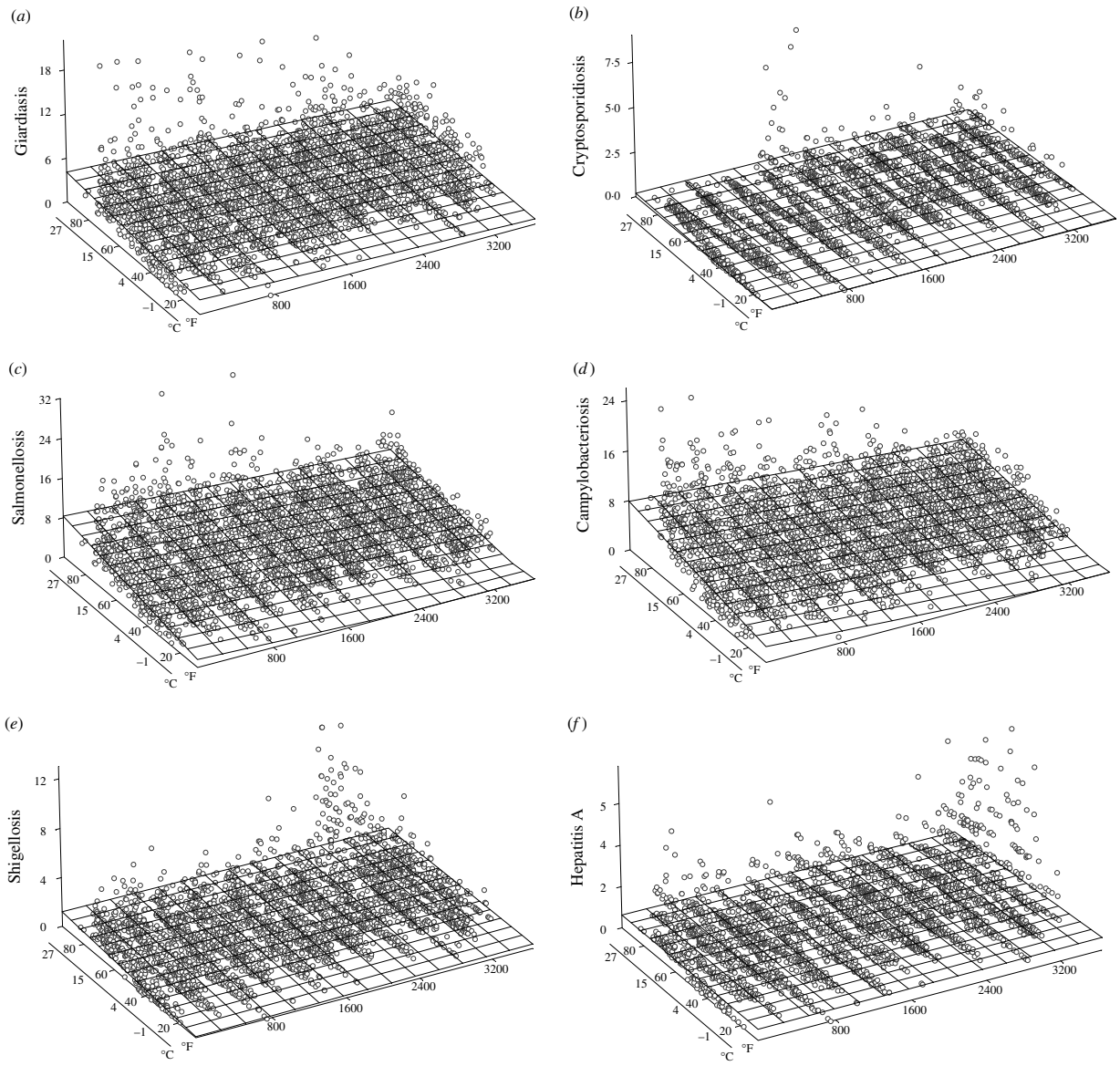

Fig. 2. Disease trend for six EDs: 3D graphical representations of disease incidence against time (in days) and ambient temperature (°C aligned with °F), which show the annual trend over 10 years for each disease.

Seasonal characteristics

The magnitude and timing of a seasonal increase, estimated from model A (for temperature) and model B (for ED) are shown in Table 2. The seasonal curve for ambient temperature peaked at the 206th ($\pm 0{\cdot}2$) day of the year (typically 24 or 25 July, week 29) with an average maximum temperature of $\sim 8{\cdot}89$ °C. Ten superimposed time series of daily values of ambient temperature together with the predicted seasonal curve are shown in Figure 3*b*. The predicted seasonal pattern for daily disease counts for each disease (Fig. 4*a*) and daily magnitude for each disease (Fig. 4*b*) are illustrated.

For the five EDs with a relationship to ambient temperature, two groups emerged. Peak *Campylobacter* incidence essentially coincided with the peak in temperature (day $208 \pm 0{\cdot}8$, $P = 0{\cdot}89$). *Salmonella* incidence peaked 13 days after the peak in ambient temperature. In another group, reported cryptosporidiosis and shigellosis peaked contemporaneously almost 1 month after the temperature peak ($242 \pm 1{\cdot}7$ and $247 \pm 1{\cdot}3$, $P < 0{\cdot}02$). Reported giardiasis peaked 1 week after cryptosporidiosis ($249 \pm 1{\cdot}2$, $P < 0{\cdot}01$), in the first week of September. The small variability in the timing of these seasonal peaks reflects the consistency of the seasonal pattern for these diseases. The variability exhibited by *Salmonella* and

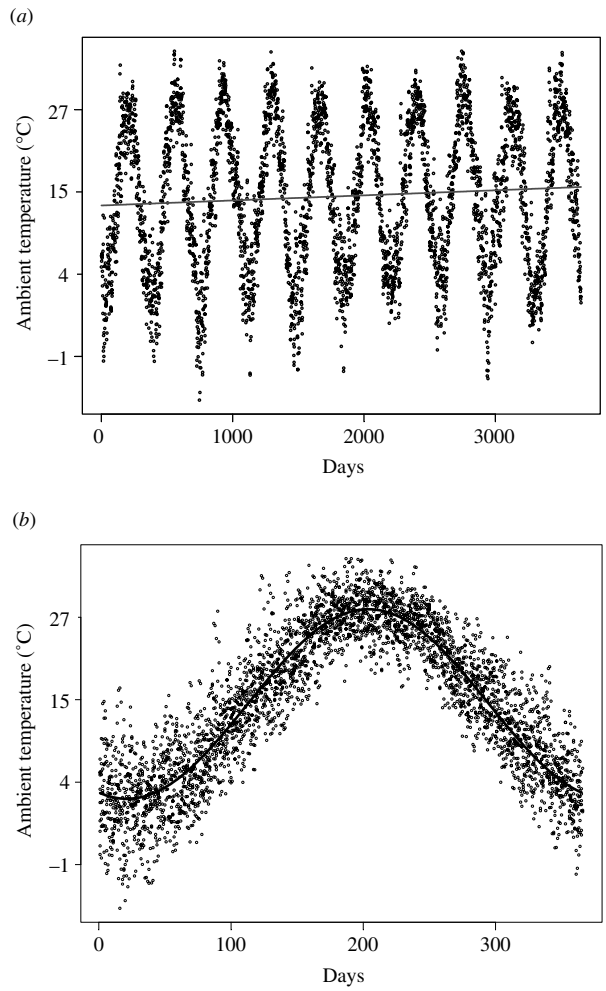

Fig. 3. Seasonal characteristics of ambient temperature. (*a*) The 10-year daily time series with the trend superimposed. (*b*) Ten years of data superimposed in one scatter plot overlaid with a fitted cosine curve to depict the systematic seasonal pattern.

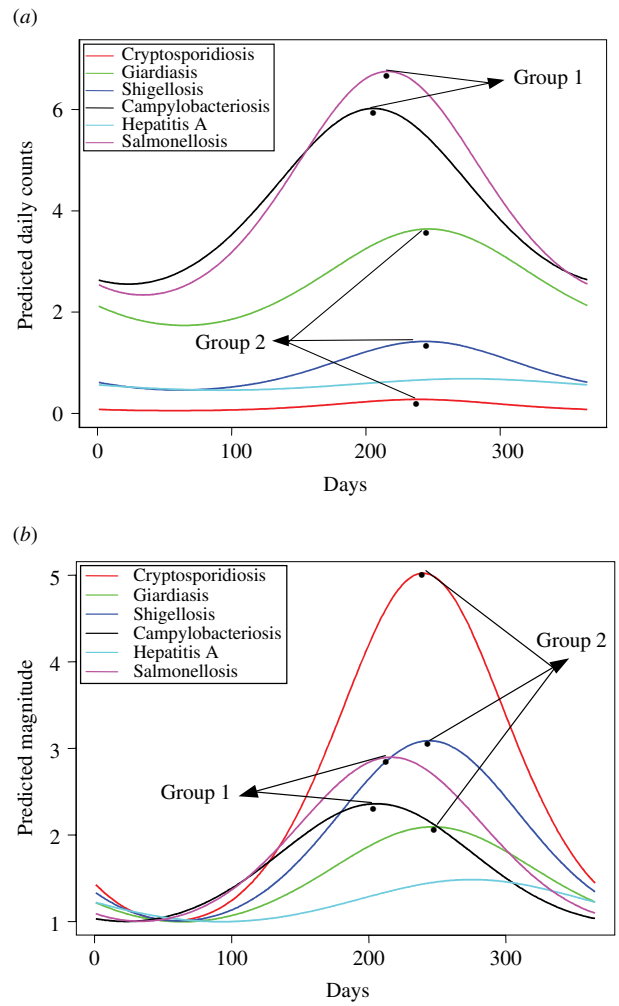

Fig. 4. Predicted seasonal pattern for (*a*) daily disease counts for each disease; (*b*) daily magnitude for each disease.

Campylobacter infections was substantially smaller than the variability exhibited by other EDs.

Unlike the other EDs, hepatitis A did not appear to have a significant systemic seasonal component as there was a large variability in the timing of the peak incidence, and only a very small percent of the variability was explained by the model (1%). The peak incidence for hepatitis A occurred in the last week of September, 63 days after the peak in temperature. As expected, the smallest peak variability was observed in the temperature curve itself.

Both parametric and non-parametric models captured strong seasonal patterns in *Salmonella* and *Campylobacter* infections with ~20% variability explained. For infections caused by *Shigella*, *Giardia*, or *Cryptosporidium*, seasonal patterns accounted for ~10% of weekly and ~8% daily variations. As expected, in the temperate climate of MA seasonality explained over 80% of variability in ambient temperature.

The results of models C and D are shown in Table 3. The predicted values for ambient temperature and for the number of cases of ED in a given week were estimated and the weeks at which those values exceeded pre-selected cut points (75th, 85th and 95th percentiles) are indicated. To demonstrate the comparability of the models we show the weeks of the seasonal maximum (in bold face) with confidence intervals (underlined), obtained in models A and B. The estimated seasonal peaks fall approximately in the middle of the shaded regions. The seasonal patterns for salmonellosis and campylobacteriosis closely follow the ambient temperature curve.

Table 3. *The predicted weekly values, the mean, and three upper percentiles (75th, 85th, and 95th), and percent variability explained by models C and D, for ambient temperature (°C) and for the number of cases of ED respectively*

Week no.	Temp. (°C)	Campylo-bacteriosis	Salmon-ellosis	Shigellosis	Crypto-sporidiosis	Giardiasis	Hepatitis A
1	3·40	2·45	2·77	0·68	0·07	2·20	0·34
2	2·18	2·97	2·73	0·56	0·03	2·11	0·57
3	1·97	2·51	2·03	0·64	0·09	1·46	0·56
4	1·72	2·46	2·19	1·13	0·10	2·03	0·44
5	1·88	3·20	2·81	0·73	0·07	2·50	0·63
6	1·83	2·64	2·39	0·54	0·04	1·94	0·50
7	4·39	2·41	2·64	0·64	0·06	1·73	0·43
8	4·56	2·83	2·53	0·53	0·07	1·69	0·46
9	4·34	2·77	2·64	0·49	0·10	2·11	0·79
10	6·16	2·84	2·59	0·49	0·14	1·96	0·61
11	6·41	2·97	2·76	0·64	0·04	2·59	0·43
12	8·86	2·94	2·59	0·73	0·06	1·70	0·47
13	11·46	3·16	2·97	0·53	0·10	2·41	0·59
14	12·13	2·69	3·23	0·39	0·06	1·91	0·43
15	12·84	3·07	3·33	0·39	0·09	2·31	0·41
16	15·91	3·40	3·10	0·34	0·13	1·70	0·39
17	16·86	3·60	3·84	0·56	0·06	2·19	0·56
18	17·72	4·07	3·71	0·30	0·06	2·19	0·54
19	18·86	3·84	3·99	0·60	0·16	2·09	0·39
20	20·10	4·19	3·66	0·59	0·07	1·66	0·39
21	21·08	4·83	4·14	0·71	0·09	1·53	0·40
22	22·76	5·89	4·64	0·87	0·11	2·49	0·59
23	24·74	5·14	5·37	0·86	0·13	2·01	0·40
24	24·75	6·91	6·19	0·66	0·10	2·27	0·39
25	26·78	6·46	6·11	0·61	0·14	2·09	0·50
26	26·67	7·01	6·46	0·80	0·19	3·34	0·53
27	27·72	7·34	6·31	0·91	0·20	2·43	0·76
28	27·95	6·74	6·24	0·94	0·10	2·94	0·53
29	27·21	6·14	6·19	1·39	0·09	3·31	0·51
30	27·29	**6·20**	6·76	1·80	0·16	3·39	0·53
31	28·22	5·29	**7·61**	1·83	0·31	3·81	0·71
32	26·14	5·51	6·87	1·70	0·34	3·64	0·74
33	25·61	5·17	7·47	1·71	0·43	4·43	0·71
34	26·51	4·57	6·67	1·67	0·41	3·53	0·70
35	25·59	5·37	7·33	**1·93**	**0·26**	4·69	0·69
36	23·72	4·46	6·09	1·30	0·49	**3·79**	0·77
37	23·19	4·40	6·01	1·46	0·20	4·51	0·77
38	20·18	3·93	5·40	1·24	0·30	3·37	**0·63**
39	18·93	4·66	5·27	1·26	0·21	3·79	0·90
40	18·06	4·17	4·54	1·04	0·34	3·31	0·70
41	16·78	4·06	4·69	0·97	0·13	3·57	0·50
42	15·90	4·04	3·77	1·11	0·16	3·06	0·54
43	14·98	4·17	3·89	0·80	0·13	2·80	0·59
44	12·73	4·19	3·27	0·97	0·09	3·09	0·79
45	10·12	3·97	3·27	0·81	0·17	2·59	0·83
46	9·65	4·09	3·59	0·81	0·14	3·23	0·81
47	8·89	3·51	2·73	0·83	0·04	2·03	0·59
48	8·85	3·47	3·97	0·87	0·11	2·01	0·40
49	6·48	2·97	3·36	0·67	0·03	2·04	0·44
50	4·56	3·20	3·23	0·79	0·19	2·17	0·43
51	4·07	2·40	2·43	0·43	0·09	1·74	0·39
52	1·99	2·41	2·99	0·43	0·07	1·81	0·61
53	−0·98	2·50	1·93	0·36	0·07	2·57	0·43

Table 3 (*cont.*)

Week no.	Temp. (°C)	Campylo-bacteriosis	Salmon-ellosis	Shigellosis	Crypto-sporidiosis	Giardiasis	Hepatitis A
Mean	14·73	4·08	4·21	0·87	0·14	2·60	0·56
75%	23·72	4·83	6·01	1·04	0·17	3·31	0·69
85%	26·22	5·59	6·26	1·32	0·22	3·54	0·75
95%	27·46	6·81	7·05	1·75	0·37	4·06	0·80
% Var	84	20	25	12	10	11	3

Bold values indicate weeks of the seasonal maximum; underlining indicates confidence intervals (obtained in models A and B). Shaded regions indicate where estimated seasonal peaks fall.

CONCLUSION

Although seasonality is a well-known phenomenon in the epidemiology of many diseases, simple analytical tools for the examination, evaluation, and comparison of seasonal patterns are limited. Analyses of disease seasonality have also been restricted by the lack of precision inherent in using monthly or weekly means. Herein we offer a framework for uniform, comprehensive, systematic, seasonality assessment via a parametric approach, using daily frequencies. This approach is highly relevant to disease surveillance, which sifts through daily frequencies of disease as well as specially designed epidemiological studies. We propose simple, easily understood characteristics for the intensity and timing of a seasonal peak. These allow us to quantify seasonality in a consistent manner and to compare relationships between diseases and environmental factors.

We applied this approach to the study of enteric diseases in MA. We found that infections caused by *Salmonella* and *Campylobacter* closely follow the ambient temperature curve. If we knew nothing else, we might hypothesize that *Salmonella* and *Campylobacter* infections share a dominant route of exposure that is strongly influenced by ambient temperature. Foodborne transmission is an obvious candidate for this route, given the capacity of *Salmonella* to grow in contaminated food and the paucity of person-to-person spread with *Campylobacter* infections. Indeed, food contamination is believed to be the most significant mode of transmission for *Salmonella* and *Campylobacter* [28–30].

In contrast, the seasonal increase in *Giardia*, *Shigella*, and *Cryptosporidium* infections form a separate cluster peaking a month after the temperature peak, strongly suggesting different route(s) of exposure than for *Salmonella* or *Campylobacter*. Reasons for this month-long temporal delay (lag) include differences in routes of transmission, amplification of infection related to person-to-person spread, survival of pathogens in the environment, incubation periods after ingestion, differences in diseases manifestation and testing practices, or combinations thereof. Outbreaks of cryptosporidiosis, giardiasis, or shigellosis associated with drinking water and recreational water use occur in the warm summer months [2, 5, 31, 32]. Hot weather leads to higher water consumption [33], promotes outdoor swimming [34], other recreational water use, and other outdoor activities. Person-to-person spread may also be increased due to the close quarters and poor hygiene of outdoor activities, such as camping or swimming, and person-to-person spread may amplify outbreaks pushing peaks to a later time period. Prior work suggests that contaminated water is a dominant source of exposure for cryptosporidiosis and giardiasis [35, 36], although foodborne transmission is certainly possible [37].

We cannot comment on the possibility that foreign travel, presence of HIV infection, specific water sources, or specific recreational water exposures were involved in these findings, as the data collected by Commonwealth of Massachusetts does not contain detailed information on these potential risk factors. The differences in seasonality between the first (*Salmonella* and *Campylobacter* infection) and the second cluster (*Giardia*, *Shigella*, and *Cryptosporidium* infections) could be in part associated with the probability of acute clinical syndromes, as well as testing and reporting practices. For each record in the database, a few dates were provided: date on event, date of disease onset, date of diagnosis, date of specimen collection, and date of reporting. We examined the differences amongst all the dates and selected the date of disease onset as the most reliable characteristic. In any passive surveillance a delay

between time of clinical manifestation and time of diagnosis and testing is practically unavoidable, however, we assume that this delay is systematic over the course of year and the lag between the peak in ambient temperature and an the peak in diseases includes this systematic component.

The seasonal pattern in cryptosporidiosis observed in this study, differs from the seasonal patterns reported by others where a slight increase in the number of positive stool tests for C*ryptosporidium parvum* and in the number of cases of cryptosporidiosis among HIV patients occurred in the spring compared with other seasons, but the difference was not statistically significant [38]. This fact could be indicative of differences in predominant routes of exposure in the HIV-infected population. If there is a spring peak in cryptosporidiosis in MA, it is not captured in the surveillance data that we analysed in this study, in part due to the fact that the highest fraction of samples for cryptosporidiosis came from children (60%) not adults. Although, the surveillance data have been shown to be underreported and oversampled in certain situations, such as during the 1995 Worcester cryptosporidiosis outbreak [14], the established surveillance system on enteric infection has valuable potential for quantifying disease trends and seasonal patterns.

In this paper we have assumed a common parametric form for seasonality, a cosine function. The shape of a cosine periodic function is defined by its shift parameter, which reflects the point of maximum amplitude, and by the length of a period, which implies that only one peak is observable in one calendar year. This assumption may not hold if a disease exhibits two seasonal peaks [39]; however, the proposed model can be extended so both peaks will be evaluated [26]. In any case, we recommend an exploration of the potential form for a seasonal pattern via nonlinear or non-parametric methods prior to modelling.

We compared our parametric approach with that of non-parametric modelling, which has an intuitive appeal and is often used for surveillance data (Table 3). The non-parametric model provides a reasonably good approximation for seasonal variation, and allows one to make a reliably independent assessment of a specific week's disease incidence against that of a reference week. However, this approach does not take into account temporal dependency, and treats each week as a separate independent category. As expected, the non-parametric model with a set of indicator variables for weeks explained a larger percentage of the variability than did the parametric model using daily counts, in part due to a lesser impact of calendar effects (holidays or day of the week effects) in weekly aggregation. However, this possible advantage is strongly diminished by the major difficulties in comparing results of non-parametric models.

For both non-parametric and parametric approaches, we utilized a Poisson regression model to predict ED incidence. Although a Poisson assumption is well suited for non-negative right-skewed outcomes, such as daily or weekly cases of infections, and can be a suitable approximation for a seasonal mean, we found the tails of the observed distributions of daily ED counts were longer than for a Poisson-like distribution. Approximation of the outcome by the Poisson distribution leads to the underestimation of predicted rates for days or weeks with very high rates, meaning that the actual degree of summer/autumn increase might be higher than predicted. We think that the model can be improved in the future by using more sophisticated tools for handling extreme values relating to outbreaks. However, until superimposed non-seasonal variation can be better predicted and identified, the selection of such tools is arbitrary.

One methodological aspect of this approach deserves special comment. The vast majority of epidemiological studies of ED seasonality have used crude quarterly or monthly aggregate data. This prevents a fully detailed, accurate, or comprehensive analysis of a seasonal pattern and may even be misleading [40]. The use of daily time series for these infections enabled us to detect significant differences in the seasonal peaks of enteric infections, which would have been lost in an analysis using monthly or weekly cumulative information. Examination of weekly rates substantially improves the evaluation of seasonal curves when compared to monthly data, but a systematic approach to the issue of week assignment in the long time series has often been lacking. The analysis of disease seasonality would benefit from the proposed approach, which can be used both as a routine in disease surveillance and as a part of specially designed epidemiological studies.

ACKNOWLEDGEMENTS

We thank the Massachusetts Department of Public Health for support throughout this project and for providing us with surveillance data. We also thank

the EPA and the National Institute of Allergy and Infectious Diseases who provided funding through grant AI43415 to E.N.N., J.G., J.K.G. and I.B.M.

DECLARATION OF INTEREST

None.

REFERENCES

1. **Amin OM.** Seasonal prevalence of intestinal parasites in the United States during 2000. *American Journal of Tropical Medicine and Hygiene* 2002; **66**: 799–803.
2. **Barwick RS, *et al.*** Surveillance for waterborne-disease outbreaks – United States, 1997–1998. *MMWR. CDC Surveillance Summaries* 2000; **49**: 1–21.
3. **Bean NH, *et al.*** Surveillance for foodborne-disease outbreaks – United States, 1988–1992. *MMWR. CDC Surveillance Summaries* 1996; **45**: 1–66.
4. **Bowman C, Flint J, Pollari F.** Canadian integrated surveillance report: *Salmonella*, *Campylobacter*, pathogenic *E. coli* and *Shigella*, from 1996 to 1999. *Canadian Communicable Disease Report* 2003; **29** (Suppl. 1): 1–6.
5. **Lee SH, *et al.*** Surveillance for waterborne-disease outbreaks – United States, 1999–2000. *MMWR. CDC Surveillance Summaries* 2002; **51**: 1–47.
6. **Levy DA, *et al.*** Surveillance for waterborne-disease outbreaks – United States, 1995–1996. *MMWR. CDC Surveillance Summaries* 1998; **47**: 1–34.
7. **Olsen SJ, *et al.*** Surveillance for foodborne-disease outbreaks – United States, 1993–1997. *MMWR. CDC Surveillance Summaries* 2000; **49**: 1–62.
8. **Addiss DG, *et al.*** Epidemiology of giardiasis in Wisconsin: increasing incidence of reported cases and unexplained seasonal trends. *American Journal of Tropical Medicine and Hygiene* 1992; **47**: 13–19.
9. **Birkhead G, Vogt RL.** Epidemiologic surveillance for endemic *Giardia lamblia* infection in Vermont. The roles of waterborne and person-to-person transmission. *American Journal of Epidemiology* 1989; **129**: 762–768.
10. **Dietz V, *et al.*** Active, multisite, laboratory-based surveillance for *Cryptosporidium parvum*. *American Journal of Tropical Medicine and Hygiene* 2000; **62**: 368–372.
11. **Furness BW, Beach MJ, Roberts JM.** Giardiasis surveillance – United States, 1992–1997. *MMWR. CDC Surveillance Summaries* 2000; **49**: 1–13.
12. **Greig JD, *et al.*** A descriptive analysis of giardiasis cases reported in Ontario, 1990–1998. *Canadian Journal of Public Health* 2001; **92**: 361–365.
13. **Majowicz SE, *et al.*** Descriptive analysis of endemic cryptosporidiosis cases reported in Ontario, 1996–1997. *Canadian Journal of Public Health* 2001; **92**: 62–66.
14. **Naumova EN, *et al.*** Use of passive surveillance data to study temporal and spatial variation in the incidence of giardiasis and cryptosporidiosis. *Public Health Report* 2000; **115**: 436–447.
15. **Hald T, Andersen JS.** Trends and seasonal variations in the occurrence of Salmonella in pigs, pork and humans in Denmark, 1995–2000. *Berliner und Munchener Tierarztliche Wochenschrift* 2001; **114**: 346–349.
16. **Patz JA, *et al.*** Effects of environmental change on emerging parasitic diseases. *International Journal of Parasitology* 2000; **30**: 1395–1405.
17. **Bentham G, Langford IH.** Climate change and the incidence of food poisoning in England and Wales. *International Journal of Biometeorology* 1995; **39**: 81–86.
18. **Bentham G, Langford IH.** Environmental temperatures and the incidence of food poisoning in England and Wales. *International Journal of Biometeorology* 2001; **45**: 22–26.
19. **Cowden JM, *et al.*** Outbreaks of foodborne infectious intestinal disease in England and Wales: 1992 and 1993. *Communicable Disease Report. CDR Review* 1995; **5**: R109–R117.
20. **Djuretic T, Wall PG, Nichols G.** General outbreaks of infectious intestinal disease associated with milk and dairy products in England and Wales: 1992 to 1996. [Erratum appears in *CDR. CDR Review* 1997; **7**: R54]. *Communicable Disease Report. CDR Review* 1997; **7**: R41–R45.
21. **Checkley W, *et al.*** Effect of El Nino and ambient temperature on hospital admissions for diarrhoeal diseases in Peruvian children. *Lancet* 2000; **355**: 442–450.
22. **Curriero FC, *et al.*** The association between extreme precipitation and waterborne disease outbreaks in the United States, 1948–1994 [see comment]. *American Journal of Public Health* 2001; **91**: 1194–1199.
23. **Smoyer KE.** A comparative analysis of heat waves and associated mortality in St. Louis, Missouri – 1980 and 1995. *International Journal of Biometeorology* 1998; **42**: 44–50.
24. **Epstein PR.** Climate change and emerging infectious diseases. *Microbes and Infection* 2001; **3**: 747–754.
25. **MacNeill IB.** A test of whether several time series share common periodicities. *Biometrika* 1977; **64**: 495–508.
26. **Naumova EN, MacNeill IB.** Seasonality assessment for biosurveillance systems. In Balakrishnan N, *et al.*, eds. *Advances in Statistical Methods for the Health Sciences: applications to cancer and AIDS studies, genome sequence analysis, and survival analysis*. Boston: Birkhauser, 2006.
27. **McCullagh P, Nelder JA.** *Generalized Linear Models*. New York: Chapman and Hall, 1989.
28. **Hobbs BC, Roberts D.** *Food Poisoning and Food Hygiene*. London: Edward Arnold, 1997.
29. **Kusumaningrum HD, *et al.*** Survival of foodborne pathogens on stainless steel surfaces and cross-contamination to foods. *International Journal of Food Microbiology* 2003; **85**: 227–236.
30. **Mead PS, *et al.*** Food-related illness and death in the United States. *Emerging Infectious Diseases* 1999; **5**: 607–625.
31. **Fleming CA, *et al.*** An outbreak of Shigella sonnei associated with a recreational spray fountain. *American Journal of Public Health* 2000; **90**: 1641–1642.
32. **Joce RE, *et al.*** An outbreak of cryptosporidiosis associated with a swimming pool. *Epidemiology and Infection* 1991; **107**: 497–508.

33. **Gofti-Laroche L, *et al.*** Description of drinking water intake in French communities (E.M.I.R.A. study) [in French]. *Revue Epidemiologique et Santé Publique* 2001; **49**: 411–422.
34. **CDC.** Surveillance data from swimming pool inspections – selected states and counties, United States, May–September 2002. *Morbidity and Mortality Weekly Report* 2003; **52**: 513–516.
35. **Rose JB, *et al.*** Climate variability and change in the United States: potential impacts on water- and foodborne diseases caused by microbiologic agents. *Environmental Health Perspectives* 2001; **109** (Suppl. 2): 211–221.
36. **Stuart JM, *et al.*** Risk factors for sporadic giardiasis: a case-control study in southwestern England. *Emerging Infectious Diseases* 2003; **9**: 229–233.
37. **Rose JB, Slifko TR.** Giardia, Cryptosporidium, and Cyclospora and their impact on foods: a review. *Journal of Food Protein* 1999; **62**: 1059–1070.
38. **Inungu JN, Morse AA, Gordon C.** Risk factors, seasonality, and trends of cryptosporidiosis among patients infected with human immunodeficiency virus. *American Journal of Tropical Medicine and Hygiene* 2000; **62**: 384–387.
39. **Naumova EN, *et al.*** Effect of precipitation on seasonal pattern variability in cryptosporidiosis recorded by the North West England surveillance system in 1990–1999. *Journal of Water and Health* 2005; **3**: 185–196.
40. **da Silva Lopes ACB.** Spurious deterministic seasonality and autocorrelation corrections with quarterly data: Further Monte Carlo results. *Empirical Economics* 1999; **24**: 341–359.